

## PROBING $\Delta$ STRUCTURE WITH PION ELECTROMAGNETIC PRODUCTION

SHIN NAN YANG

*Physics Department, National Taiwan University  
 Taipei 10617, Taiwan*

SABIT S. KAMALOV

*Bogoliubov Laboratory for Theoretical Physics, JINR  
 Dubna, 141980 Moscow Region, Russia*

The Dubna-Mainz-Taipei dynamical model for pion electromagnetic production, which can describe well the existing data from threshold up to 1 GeV photon lab energy, is presented and used to analyze the recent precision data in the  $\Delta$  region. We find that, within our model, the bare  $\Delta$  is almost spherical while the physical  $\Delta$  is oblate. The deformation is almost saturated by the pion cloud effects. We further find that up to  $Q^2 = 4.0(\text{GeV}/c)^2$ , the extracted helicity amplitude  $A_{3/2}$  and  $A_{1/2}$  remain comparable with each other, implying that hadronic helicity is not conserved at this range of  $Q^2$ . The ratio  $E_{1+}/M_{1+}$  obtained show, starting from a small and negative value at the real photon point, a clear tendency to cross zero, and to become positive with increasing  $Q^2$ . This is a possible indication of a very slow approach toward the pQCD region. Finally, we find that the bare helicity amplitude  $A_{1/2}$  and  $S_{1/2}$ , but not  $A_{3/2}$ , starts exhibiting the scaling behavior at about  $Q^2 \geq 2.5(\text{GeV}/c)^2$ .

### 1. Introduction

$\Delta$  is the first excited state of the nucleon and the only well isolated nucleon resonance. Its properties serve as a bench mark for models of nucleon structure. It is hence important to extract  $\Delta$ 's properties from experiments reliably.

There are two kinds of electromagnetic properties of the  $\Delta$ . The first involves the  $\Delta$  itself, like the magnetic dipole moment  $\mu_\Delta$  and electric quadrupole moment  $Q_\Delta$ . They are difficult to measure because of the short life time of the  $\Delta$ . The others involve the  $N \rightarrow \Delta$  transition, like  $\mu_{N \rightarrow \Delta}$  and  $Q_{N \rightarrow \Delta}$ . They can be determined from the pion electromagnetic production via the following relations,

$$\mu_{N \rightarrow \Delta} = -\frac{m_N}{2\sqrt{\pi\alpha_e\omega}}(A_{1/2}^\Delta + \sqrt{3}A_{3/2}^\Delta), \quad (1)$$

$$Q_{N \rightarrow \Delta} = -\frac{3}{2\sqrt{\pi\alpha_e\omega^3}}(A_{1/2}^\Delta - \frac{1}{\sqrt{3}}A_{3/2}^\Delta), \quad (2)$$

where  $A$ 's are the helicity amplitudes and  $\omega$  the photon energy.

In this talk, we'll focus mostly on the  $\Delta$  properties associated with the  $\gamma^* N \leftrightarrow \Delta$  transition. They are of interest because in symmetric  $SU(6)$  quark models and with the inclusion of only one-body current contribution <sup>1</sup>, the  $\gamma N \Delta$  transition can proceed only via the flip of a single quark spin in the nucleon, leading to  $M_{1+}$  dominance and  $E_{1+} = S_{1+} \equiv 0$ . If the  $\Delta$  is deformed, then the photon can excite a nucleon into a  $\Delta$  through electric quadrupole E2 and Coulomb quadrupole C2 transitions. Recent experiments give nonvanishing ratio  $R_{EM} = E_{1+}^{(3/2)} / M_{1+}^{(3/2)}$  lying between  $-2.5\%$  <sup>2</sup> and  $-3.0\%$  <sup>3</sup>, or equivalently  $Q_{N \rightarrow \Delta} \simeq -0.108 \text{ fm}^2$ , at  $Q^2 = 0$ . This has been widely taken as an indication of a deformed (oblate)  $\Delta$ , namely, an admixture of a D state in the  $\Delta$ . On the other hand, in the limit of  $Q^2 \rightarrow \infty$ , pQCD predicts the dominance of helicity-conserving amplitudes <sup>4</sup> and scaling results <sup>5,6</sup>. The hadronic helicity conservation should have the consequence that  $R_{EM}$  approaches 1. The scaling behavior predicted by pQCD for the helicity amplitudes is  $A_{1/2}^\Delta \sim Q^{-3}$ ,  $A_{3/2}^\Delta \sim Q^{-5}$ , and the Coulomb helicity amplitude  $S_{1/2}^\Delta \sim Q^{-3}$ , resulting in  $R_{SM} = S_{1+}^{(3/2)} / M_{1+}^{(3/2)} \rightarrow \text{const}$ . Accordingly, the question of how  $R_{EM}$  would evolve from a very small negative value at  $Q^2 = 0$  to  $+100\%$  at sufficiently high  $Q^2$ , has attracted great interest both theoretically and experimentally.

Because of the significance of the physics involved in the  $Q^2$  evolution of  $R_{EM}$  and  $R_{SM}$ , it is important to employ the best possible extraction method in the analysis of the data. So we now turn to the theoretical method in describing the pion electromagnetic production.

## 2. Dynamical Model for Pion Electromagnetic Production

At present, there exist three different theoretical methods to describe the pion electromagnetic production. The oldest one is the dispersion theory which was developed by Chew *et al.* <sup>7</sup>, and is still in use today <sup>8</sup>. It is based on analyticity, unitarity and crossing symmetry. The second method was based on chiral Lagrangians as carried out by Olsson and Osypowski <sup>9</sup>. This work was further developed by Davidson *et al.* <sup>10</sup>. MAID <sup>11</sup> is also constructed along this line. In 1985, Yang <sup>12</sup> and Tanabe and Ohta <sup>13</sup> developed the dynamical model of pion photoproduction which has been currently in wide use <sup>14,15,16,17</sup>. We have recently constructed a DMT dynamical model <sup>18,19</sup> which can describe the existing pion production data from threshold <sup>20</sup> to  $1 \text{ GeV}$  photon lab energy. We will use DMT model for our analysis hereafter.

In the dynamical approach to pion photo- and electroproduction <sup>12</sup>, the t-matrix can be expressed as

$$t_{\gamma\pi}(E) = v_{\gamma\pi} + v_{\gamma\pi} g_0(E) t_{\pi N}(E), \quad (3)$$

and the physical multipoles in channel  $\alpha$  are given by

$$\begin{aligned} t_{\gamma\pi}^{(\alpha)}(q_E, k; E + i\epsilon) &= \exp(i\delta^{(\alpha)}) \cos \delta^{(\alpha)} \\ &\times \left[ v_{\gamma\pi}^{(\alpha)}(q_E, k) + P \int_0^\infty dq' \frac{q'^2 R_{\pi N}^{(\alpha)}(q_E, q') v_{\gamma\pi}^{(\alpha)}(q', k)}{E - E_{\pi N}(q')} \right], \end{aligned} \quad (4)$$

where  $v_{\gamma\pi}$  is the transition potential for  $\gamma^* N \rightarrow \pi N$ , and  $t_{\pi N}$  and  $g_0$  denote the  $\pi N$

scattering t-matrix and free propagator, respectively, with  $E \equiv W$  the total energy in the CM frame.  $\delta^{(\alpha)}$  and  $R_{\pi N}^{(\alpha)}$  are the  $\pi N$  scattering phase shift and reaction matrix in channel  $\alpha$ , respectively;  $q_E$  is the pion on-shell momentum and  $k = |\mathbf{k}|$  is the photon momentum.

In a resonant channel like (3,3) in which the  $\Delta(1232)$  plays a dominant role, the transition potential  $v_{\gamma\pi}$  consists of two terms

$$v_{\gamma\pi}(E) = v_{\gamma\pi}^B + v_{\gamma\pi}^\Delta(E), \quad (5)$$

where  $v_{\gamma\pi}^B$  is the background transition potential and  $v_{\gamma\pi}^\Delta(E)$  corresponds to the contribution of the bare  $\Delta$  excitation. The resulting t-matrix can be decomposed into two terms<sup>18</sup>

$$t_{\gamma\pi}(E) = t_{\gamma\pi}^B(E) + t_{\gamma\pi}^\Delta(E), \quad (6)$$

where

$$t_{\gamma\pi}^B(E) = v_{\gamma\pi}^B + v_{\gamma\pi}^B g_0(E) t_{\pi N}(E), \quad (7)$$

$$t_{\gamma\pi}^\Delta(E) = v_{\gamma\pi}^\Delta + v_{\gamma\pi}^\Delta g_0(E) t_{\pi N}(E). \quad (8)$$

Here  $t_{\gamma\pi}^B$  includes the contributions from the nonresonant background and renormalization of the vertex  $\gamma^* N \Delta$ . The advantage of such a decomposition is that all the processes which start with the excitation of the bare  $\Delta$  are summed up in  $t_{\gamma\pi}^\Delta$ . Note that the multipole decomposition of both  $t_{\gamma\pi}^B$  and  $t_{\gamma\pi}^\Delta$  would take the same form as Eq. (4).

As in MAID<sup>11</sup>, the background potential  $v_{\gamma\pi}^{B,\alpha}(W, Q^2)$  was described by Born terms obtained with an energy dependent mixing of pseudovector-pseudoscalar  $\pi NN$  coupling and t-channel vector meson exchanges. The mixing parameters and coupling constants were determined from an analysis of nonresonant multipoles in the appropriate energy regions. In the new version of MAID, the  $S$ ,  $P$ ,  $D$  and  $F$  waves of the background contributions are unitarized in accordance with the K-matrix approximation,

$$t_{\gamma\pi}^{B,\alpha}(\text{MAID}) = \exp(i\delta^{(\alpha)}) \cos \delta^{(\alpha)} v_{\gamma\pi}^{B,\alpha}(W, Q^2). \quad (9)$$

From Eqs. (4) and (9), one finds that the difference between the background terms of MAID and of the dynamical model is that off-shell rescattering contributions (principal value integral) are not included in MAID. With  $v_{\gamma\pi}^{B,\alpha}$  specified,  $t_{\gamma\pi}^{B,\alpha}$  can be evaluated according to Eq. (4) with a model for the reaction matrix  $R_{\pi N}^\alpha$ . This is done with a meson-exchange pion-nucleon model we have constructed<sup>21</sup> within Bethe-Salpeter formulation. To take into account of the inelastic effects at the higher energies, we replace  $\exp(i\delta^{(\alpha)}) \cos \delta^{(\alpha)} = \frac{1}{2}[\exp(2i\delta^{(\alpha)}) + 1]$  in Eq. (4) by  $\frac{1}{2}[\eta_\alpha \exp(2i\delta^{(\alpha)}) + 1]$ , where  $\eta_\alpha$  is the inelasticity. In our actual calculations, both the  $\pi N$  phase shifts  $\delta^{(\alpha)}$  and inelasticity parameters  $\eta_\alpha$  are taken from the analysis of the GWU group<sup>22</sup>.

Following Ref. 11, we assume a Breit-Wigner form for the resonance contribution  $t_{\gamma\pi}^{R,\alpha}(W, Q^2)$  to the total multipole amplitude,

$$t_{\gamma\pi}^{R,\alpha}(W, Q^2) = \bar{A}_\alpha^R(Q^2) \frac{f_{\gamma R}(W) \Gamma_R M_R f_{\pi R}(W)}{M_R^2 - W^2 - i M_R \Gamma_R} e^{i\phi}, \quad (10)$$

*Probing  $\Delta$  structure...*

where  $f_{\pi R}$  is the usual Breit-Wigner factor describing the decay of a resonance  $R$  with total width  $\Gamma_R(W)$  and physical mass  $M_R$ . The expressions for  $f_{\gamma R}$ ,  $f_{\pi R}$  and  $\Gamma_R$  are given in Ref. <sup>11</sup>. The phase  $\phi(W)$  in Eq. (10) is introduced to adjust the phase of the total multipole to equal the corresponding  $\pi N$  phase shift  $\delta^{(\alpha)}$ . Because  $\phi = 0$  at resonance,  $W = M_R$ , this phase does not affect the  $Q^2$  dependence of the  $\gamma NR$  vertex.

### 3. Results and Discussions

We now concentrate on the  $\Delta(1232)$  resonance. In this case the magnetic dipole ( $\bar{A}_M^\Delta$ ), the electric ( $\bar{A}_E^\Delta$ ) and Coulomb ( $\bar{A}_S^\Delta$ ) quadrupole form factors are related to the conventional electromagnetic helicity amplitudes  $A_{1/2}^\Delta$ ,  $A_{3/2}^\Delta$  and  $S_{1/2}^\Delta$  by

$$\bar{A}_M^\Delta(Q^2) = -\frac{1}{2}(A_{1/2}^\Delta + \sqrt{3}A_{3/2}^\Delta), \quad (11)$$

$$\bar{A}_E^\Delta(Q^2) = \frac{1}{2}(-A_{1/2}^\Delta + \frac{1}{\sqrt{3}}A_{3/2}^\Delta), \quad (12)$$

$$\bar{A}_S^\Delta(Q^2) = -\frac{S_{1/2}^\Delta}{\sqrt{2}}. \quad (13)$$

We stress that the physical meaning of these resonant amplitudes in different models is different <sup>16,18</sup>. In MAID, they contain contributions from the background excitation and describe the so called "dressed"  $\gamma N \Delta$  vertex. However, in the dynamical model the background excitation is included in  $t_{\gamma\pi}^{B,\alpha}$  and the electromagnetic vertex  $\bar{A}_\alpha^\Delta(Q^2)$  corresponds to the "bare" vertex.

We further write, for electric ( $\alpha = E$ ), magnetic ( $\alpha = M$ ) and Coulomb ( $\alpha = S$ ) multipoles,

$$\bar{A}_\alpha^\Delta(Q^2) = X_\alpha^\Delta(Q^2) \bar{A}_\alpha^\Delta(0) \frac{k}{k_W} F(Q^2), \quad (14)$$

where  $k_W = (W^2 - m_N^2)/2W$ ,  $k^2 = Q^2 + ((W^2 - m_N^2 - Q^2)/2W)^2$ . The form factor  $F$  is taken to be  $F(Q^2) = (1 + \beta Q^2) e^{-\gamma Q^2} G_D(Q^2)$ , where  $G_D(Q^2) = 1/(1+Q^2/0.71)^2$  is the usual dipole form factor. The parameters  $\beta$  and  $\gamma$  were determined by fitting  $\bar{A}_M^\Delta(Q^2)$  to the data for  $G_M^*$  defined by <sup>11,18,23</sup>,  $M_{1+}^{(3/2)}(M_\Delta, Q^2) = (k/m_N)\sqrt{3\alpha_e/8\Gamma_{exp}q_\Delta} G_M^*(Q^2)$ , where  $\alpha_e = 1/137$ ,  $\Gamma_{exp} = 115$  MeV, and  $q_\Delta$  is the pion momentum at  $W = M_\Delta$ . The values of  $\bar{A}_M^\Delta(0)$  and  $\bar{A}_E^\Delta(0)$  were determined by fitting to the multipoles obtained in the recent analyses of the Mainz <sup>8</sup> and GWU <sup>22</sup> groups. Both  $X_E$  and  $X_S$  are to be determined by the experiment with  $X_\alpha^\Delta(0) = 1$ .

#### 3.1. Pion Photoproduction ( $Q^2 = 0$ )

With background  $t_{\gamma\pi}^B$ , and the resonance contributions associated with  $\Delta(1232)$  and other resonances determined, we obtain excellent agreement with the existing pion photoproduction data, including cross sections and polarization data, from threshold <sup>20</sup> up to 1 GeV photon lab energy <sup>25</sup>. Our results for  $M_{1+}^{(3/2)}$  and  $E_{1+}^{(3/2)}$  multipoles at  $Q^2 = 0$  are shown in Fig. 1 by solid curves. The dashed curves

denote the contribution from  $t_{\gamma\pi}^B$  only. The dotted curves represent the K-matrix approximation to  $t_{\gamma\pi}^B$ , namely, without the principal value integral term included.

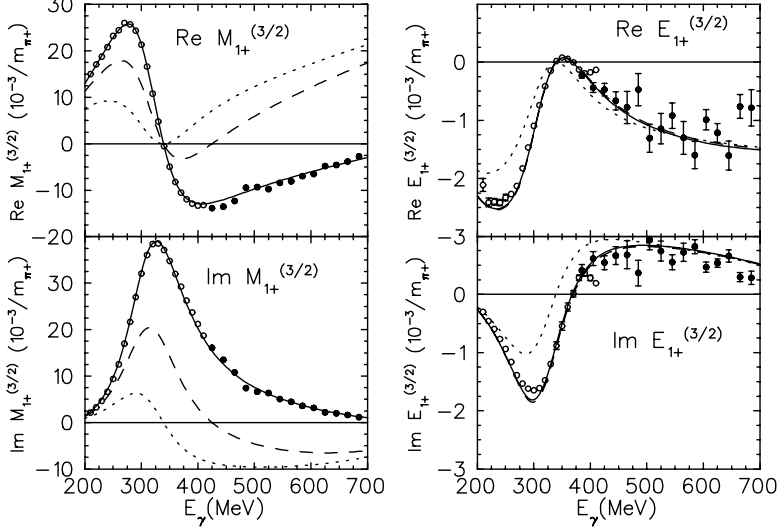


Fig. 1. Real and imaginary parts of the  $M_{1+}^{(3/2)}$  and  $E_{1+}^{(3/2)}$  multipoles. Dotted and dashed curves are the results for the  $t_{\gamma\pi}^B$  obtained without and with principal value integral contribution in Eq. (4), respectively. Solid curves are the full results with bare  $\Delta$  excitation. For the  $E_{1+}$  dashed and solid curves are practically the same due to the small value of the bare  $\bar{A}_E^\Delta$ . The open and full circles are the results from the Mainz dispersion relation analysis<sup>8</sup> and from the VPI analysis<sup>22</sup>, respectively.

The numerical values obtained for  $\bar{A}_M^\Delta$  and  $\bar{A}_E^\Delta$ , the helicity amplitudes, and  $\mu_{N \rightarrow \Delta}$  and  $Q_{N \rightarrow \Delta}$  at  $Q^2 = 0$ , are given in Table 1 along with the corresponding "dressed" values. At the resonance position  $t_{\gamma\pi}^B$  vanishes within K-matrix approximation and only principal value integral term survives. The latter corresponds to the contribution where  $\Delta$  is excited by the pion produced via  $v_{\gamma\pi}^B$ . Consequently, the addition of this contribution to  $t_{\gamma\pi}^\Delta$  can be considered as a dressing of the  $\gamma N \Delta$  vertex. The dressed helicity amplitudes obtained in this way are in very good agreements with PDG values.

Table 1. Comparison of the "bare" and "dressed" values for the amplitudes  $\bar{A}^\Delta$ , ( $10^{-3} \text{ GeV}^{-1/2}$ ),  $\mu_{N \rightarrow \Delta}$  ( $\mu_N$ ), and  $Q_{N \rightarrow \Delta}$  ( $\text{fm}^2$ ) as compared with PDG values.

	$\bar{A}_M^\Delta$	$\bar{A}_E^\Delta$	$A_{1/2}^\Delta$	$A_{3/2}^\Delta$	$\mu_{N \rightarrow \Delta}$	$Q_{N \rightarrow \Delta}$
"bare"	$158 \pm 2$	$0.4 \pm 0.3$	$-80 \pm 2$	$-136 \pm 3$	1.922	0.009
"dressed"	$289 \pm 2$	$-7 \pm 0.4$	$-134 \pm 2$	$-256 \pm 2$	3.516	-0.081
PDG	$293 \pm 8$	$-4.5 \pm 4.2$	$-140 \pm 5$	$-258 \pm 6$	3.512	-0.072

One notices that the bare values for the magnetic helicity amplitudes determined above, which amount to only about 60% of the corresponding dressed values, are

*Probing  $\Delta$  structure...*

close to the predictions of the constituent quark model (CQM). The large reduction of the helicity amplitudes from the dressed to the bares ones result from the fact that the principal value integral part of Eq. (4), which represents the effects of the off-shell pion rescattering, contributes approximately for half of the  $M_{1+}$  as indicated by the dashed curves in Fig. 1.

For the standard Sach-type form factor  $G_M^\Delta(0)$ <sup>26</sup>, which is proportional to  $\mu_{N \rightarrow \Delta}(0)$ , our bare and dressed values are  $1.65 \pm 0.02$  and  $3.06 \pm 0.02$ , respectively. On the other hand, results of CQM calculations lie in the range 1.4–2.2<sup>27</sup>. From this result we conclude that pion rescattering is the main mechanism responsible for the longstanding discrepancy in the description of the magnetic  $\gamma^* N \rightarrow \Delta$  transition within CQM.

For  $E_{1+}^{(3/2)}$ , the dominance of background and pion rescattering contributions further leads to a very small bare values for electric transition and  $Q_{N \rightarrow \Delta}$ . It implies that the bare  $\Delta$  is almost spherical. We further note that the dressed value for  $Q_{N \rightarrow \Delta}$  is also small, negative but finite. Since it is known<sup>28,29,30</sup> that  $Q_{N \rightarrow \Delta}$  is proportional to  $Q_\Delta$ , we conclude that the physical  $\Delta$  is oblate.

### 3.2. Pion Electroproduction ( $Q^2 \neq 0$ )

The DMT model is used to analyze the recent JLab differential cross section data<sup>31</sup> on  $p(e, e'p)\pi^0$  at high  $Q^2$ . All measured data, 751 points at  $Q^2 = 2.8$  and 867 points at  $Q^2 = 4.0$  ( $\text{GeV}/c$ )<sup>2</sup> covering the entire energy range  $1.1 < W < 1.4$   $\text{GeV}$ , are included in our global fitting procedure. We obtain a very good fit to the measured differential cross sections<sup>19</sup>. In fact, the values of  $\chi^2/d.o.f.$  for model are smaller<sup>19</sup> than those obtained in Ref. <sup>31</sup>. Our results for the  $G_M^*$  form factor are shown in Fig. 2. Here the best fit is obtained with  $\gamma = 0.42$  ( $\text{GeV}/c$ )<sup>-2</sup> and  $\beta = 0.61$  ( $\text{GeV}/c$ )<sup>-2</sup>.

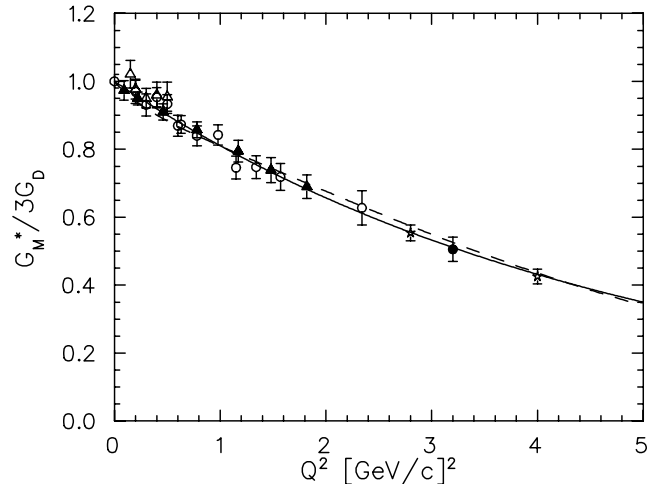


Fig. 2. The  $Q^2$  dependence of the  $G_M^*$  form factor. The solid and dashed curves are the results of the MAID and DMT analyses, respectively. The data at  $Q^2 = 2.8$  and  $4.0$  ( $\text{GeV}/c$ )<sup>2</sup> are from Ref.<sup>31</sup>, other data from Refs.<sup>24</sup>.

With the resonance parameters  $X_\alpha^\Delta(Q^2)$  determined from the fit, the ratios  $R_{EM}$

and  $R_{SM}$  of the total multipoles and the helicity amplitudes  $A_{1/2}$  and  $A_{3/2}$  can then be calculated at resonance. We perform the calculations for both physical ( $p\pi^0$ ) and isospin 3/2 channels and find them to agree with each other. The extracted  $Q^2$  dependence of the  $X_\alpha^\Delta$  parameters is:  $X_E^\Delta = 1 + Q^4/2.4$ ,  $X_S^\Delta = 1 - 10Q^2$ , with  $Q^2$  in units  $(\text{GeV}/c)^2$ .

Our extracted values for  $R_{EM}$  and  $R_{SM}$  and a comparison with the results of Ref. <sup>31</sup> are shown in Fig. 3. The main difference between our results and those of Ref. <sup>31</sup> is that our values of  $R_{EM}$  show a clear tendency to cross zero and change sign as  $Q^2$  increases. This is in contrast with the results obtained in the original analysis <sup>31</sup> of the data which concluded that  $R_{EM}$  would stay negative and tend toward more negative values with increasing  $Q^2$ . Furthermore, we find that

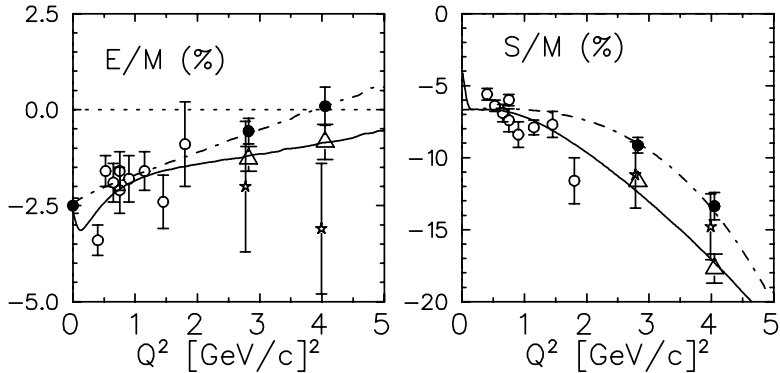


Fig. 3. The  $Q^2$  dependence of the ratios  $R_{EM}^{(p\pi^0)}$  and  $R_{SM}^{(p\pi^0)}$  at  $W = 1232$  MeV. The solid and dash-dotted curves are the DMT and MAID results, respectively. Results of previous data analysis at  $Q^2 = 0$  from Ref.<sup>2</sup>, data at  $Q^2 = 2.8$  and  $4.0$   $(\text{GeV}/c)^2$  from Ref.<sup>31</sup> (stars). Results of our analysis at  $Q^2 = 2.8$  and  $4.0$   $(\text{GeV}/c)^2$  are obtained using MAID ( $\bullet$ ) and the dynamical models ( $\Delta$ ). Open cycles are from Ref.<sup>32</sup>.

the absolute value of  $R_{SM}$  is strongly increasing. Note that very recently similar results were obtained by SAID group <sup>33</sup>.

At low  $Q^2$ , the  $Q^2$  evolution of both  $R_{EM}$  and  $R_{SM}$  obtained with DMT and MAID exhibits some marked difference, as can be seen in Fig. 3. In particular, the value of  $R_{SM}$  at  $Q^2 = 0$  extracted with these two models even differ by a factor of 2. This is due to the fact that within MAID, the background contribution of Eq. (9) vanishes at the resonance so that  $R_{EM}$  and  $R_{SM}$  become the ratios of the dressed form factors  $\bar{A}_\alpha^\Delta$ . Therefore, if we neglect the small influence of the  $X_\alpha^\Delta(Q^2)$  factor at small  $Q^2$ , this leads to a rather smooth  $Q^2$  dependence for the  $R_{EM}$  and  $R_{SM}$ . In the DMT model, both  $E_{1+}^{(3/2)}$  and  $S_{1+}^{(3/2)}$  are dominated by the contribution from pion cloud <sup>18</sup>, namely, the principal value integral term in Eq. (4). Our results indicate that the  $Q^2$  dependence of the pion cloud contribution produces negative slope at small  $Q^2$ . It is interesting to observe that the recent calculation of the two-body current contribution, which in part includes the pion cloud effect, to the  $R_{SM}$  within a constituent quark model <sup>1</sup> also gives results for  $R_{SM}$  similar to our DMT values at small  $Q^2$ . Similar effects were observed also in Refs. <sup>34,35</sup>.

In terms of helicity amplitudes, our results for a small  $R_{EM}$  can be understood

Probing  $\Delta$  structure...

in that the extracted  $A_{3/2}$  remains as large as the helicity conserving  $A_{1/2}$  up to  $Q^2 = 4.0(\text{GeV}/c)^2$ , as seen in Fig. 4, resulting in a small  $E_{1+}$ . The contributions from the bare  $\Delta$  and pion cloud obtained with DMT are also shown by the dashed and dotted curves, respectively. Note that the latter drop faster than the bare  $\Delta$  contribution.

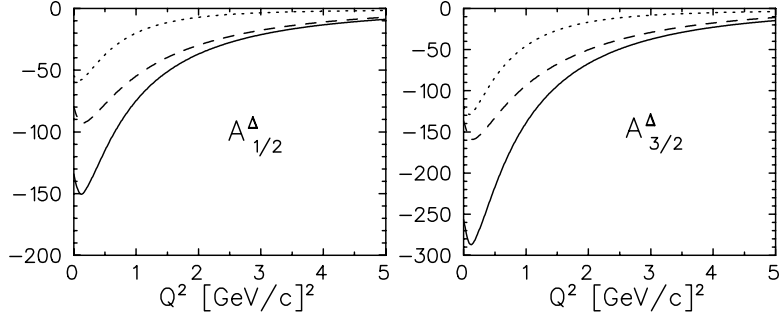


Fig. 4. The  $Q^2$  dependence of the bare (dashed curves) and dressed (solid curves) helicity amplitudes  $A_{1/2}^{\Delta}$  and  $A_{3/2}^{\Delta}$  (in units  $10^{-3} \text{ GeV}^{-1/2}$ ) extracted with DMT. The dotted curves are the pion cloud contributions.

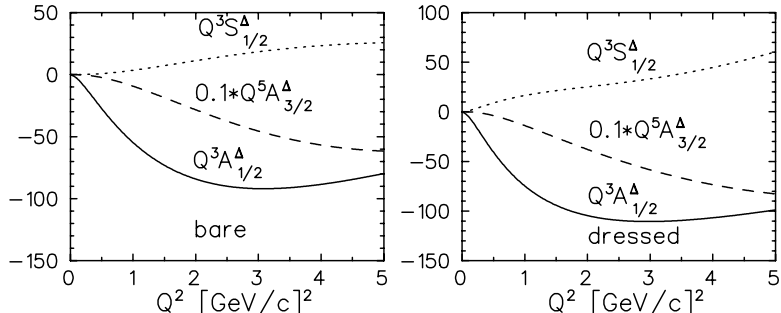


Fig. 5. The  $Q^2$  dependence of the  $Q^3 A_{1/2}^{\Delta}$  (solid curve)  $Q^5 A_{3/2}^{\Delta}$  (dashed curve) and  $Q^3 S_{1/2}^{\Delta}$  (dotted curve) amplitudes (in units  $10^{-3} \text{ GeV}^{n/2}$ ) obtained with DMT.

Finally, we present in Fig. 5 our DMT results for  $Q^3 A_{1/2}^{\Delta}$ ,  $Q^5 A_{3/2}^{\Delta}$ , and  $Q^3 S_{1/2}^{\Delta}$  to check the scaling behaviour of the bare and dressed helicity amplitudes. Note that the scaling behavior predicted by pQCD arises from the 3 quark (3q) Fock states in the nucleon and  $\Delta$  and should apply primarily to the bare amplitudes. We find that the bare  $S_{1/2}^{\Delta}$  and  $A_{1/2}^{\Delta}$  clearly starts exhibiting the pQCD scaling behavior at about  $Q^2 \geq 2.5(\text{GeV}/c)^2$ . However, it is difficult to draw any definite conclusion for  $Q^5 A_{3/2}^{\Delta}$ . The dressed Coulomb form factor  $S_{1/2}^{\Delta}$  does not exhibit pQCD scaling behavior in the considered  $Q^2$ -range. This is due to the fact that in this case the dominant pion cloud contribution does not drop as fast as in the transverse amplitudes. From these results, it appears likely that scaling will set in earlier than the helicity conservation. This is not surprising in the sense that the pQCD scaling behavior is predicted based on the argument that, in exclusive reactions,

when the photon finds the nucleon in a small  $3q$  Fock substate, with dimensions comparable to the photon wavelength, then processes with only two hard gluon exchanges dominate<sup>6</sup>. On the other hand, hadron helicity would be conserved only if this small  $3q$  Fock state would further have a spherically symmetric distribution amplitude such that  $L_z = 0$  and the hadron helicity is the sum of individual quark helicities.

#### 4. Summary

In summary, we have studied the  $\Delta$  structure by re-analyzing the recent JLab data for electroproduction of the  $\Delta(1232)$  resonance via  $p(e, e'p)\pi^0$  with the DMT dynamical model for pion electroproduction, which give excellent descriptions of the existing data. Our results indicate that the bare  $\Delta$  is almost spherical and hence very difficult to be directly excited via electric E2 and Coulomb C2 quadrupole excitations. The experimentally observed  $E_{1+}^{(3/2)}$  and  $S_{1+}^{(3/2)}$  multipoles are, to a very large extent, saturated by the contribution from pion cloud, i.e., pion rescattering effects. The negative value for the "dressed" value of  $Q_{N \rightarrow \Delta}$  can be interpreted that the physical  $\Delta$  is oblate. We find that  $A_{3/2}^{\Delta}$  is still as large as  $A_{1/2}^{\Delta}$  at  $Q^2 = 4$   $(\text{GeV}/c)^2$ , which implies that hadronic helicity conservation is not yet observed in this region of  $Q^2$ . Accordingly, our extracted values for  $R_{EM}$  are still far from the pQCD predicted value of +100%. However, in contrast to previous results we find that  $R_{EM}$ , starting from a small and negative value at the real photon point, actually exhibits a clear tendency to cross zero and change sign as  $Q^2$  increases, while the absolute value of  $R_{SM}$  is strongly increasing. In regard to the scaling, our analysis indicates that bare  $S_{1/2}^{\Delta}$  and  $A_{1/2}^{\Delta}$ , but not  $A_{3/2}^{\Delta}$ , starts exhibiting the pQCD scaling behavior at about  $Q^2 \geq 2.5(\text{GeV}/c)^2$ . It appears likely that the onset of scaling behavior might take place at a lower momentum transfer than that of hadron helicity conservation.

#### Acknowledgments

Part of the results presented here were obtained in collaboration with O. Hanstein, D. Drechsel, and L. Tiator. This work is supported in part by the National Science Council of the Republic of China under grant No. NSC 91-2112-M002-023.

#### References

1. P. Grabmayr and A. J. Buchmann, *Phys. Rev. Lett.* **86**, 2237 (2001).
2. R. Beck *et al.* *Phys. Rev. Lett.* **78**, 606 (1997).
3. G. Blanpied *et al.* *Phys. Rev. Lett.* **79**, 4337 (1997).
4. S. J. Brodsky and G. P. Lepage, *Phys. Rev. D* **23**, 1152 (1981); *ibid.* **24**, 2848 (1981).
5. C. E. Carlson, *Phys. Rev. D* **34**, 2704 (1986); C. E. Carlson and N. C. Mukhopadhyay, *Phys. Rev. Lett.* **81**, 2446 (1998).
6. P. Stoler, *Phys. Rev. D* **44**, 73 (1991); *Phys. Rep.* **226**, 103 (1993); G. Sterman and P. Stoler, *Annu. Rev. Nucl. Sci.* **47**, 193 (1997).
7. G. F. Chew, M. L. Goldberger, F. E. Low, and Y. Nambu, *Phys. Rev.* **106**, 1345 (1957).
8. O. Hanstein, D. Drechsel, and L. Tiator, *Nucl. Phys.* **A632**, 561 (1998).
9. M. G. Olsson and E. T. Osypowski, *Nucl. Phys.* **B87**, 399 (1975).

*Probing  $\Delta$  structure...*

10. R. M. Davidson, N. C. Mukhopadhyay, and R. S. Wittman, *Phys. Rev. D* **43**, 71 (1991).
11. D. Drechsel, O. Hanstein, S. S. Kamalov and L. Tiator, *Nucl. Phys. A* **645**, 145 (1999).
12. S. N. Yang, *J. Phys. G* **11**, L205 (1985).
13. H. Tanabe and K. Ohta, *Phys. Rev. C* **31**, 1876 (1985).
14. S. Nozawa, B. Blankleider, and T.-S. H. Lee, *Nucl. Phys. A* **513**, 459 (1990).
15. Y. Surya and F. Gross, *Phys. Rev. C* **53**, 2422 (1996).
16. T. Sato and T.-S. H. Lee, *Phys. Rev. C* **54**, 2660 (1996).
17. S. N. Yang, *Chin. J. Phys.* **34**, 984 (1996); S. S. Hsiao, C. T. Hung, J. L. Tsai, S. N. Yang, and Y. B. Dong, *Few-Body Systems* **25**, 55 (1998).
18. S. S. Kamalov and S. N. Yang, *Phys. Rev. Lett.* **83**, 4494 (1999).
19. S. S. Kamalov, S. N. Yang, D. Drechsel, O. Hanstein, and L. Tiator, *Phys. Rev. C* **64**, 032201 (2001).
20. S. S. Kamalov, G. Y. Chen, S. N. Yang, D. Drechsel, and L. Tiator, *Phys. Lett.* **B522**, 27 (2001).
21. C. T. Hung, S. N. Yang and T.-S. H. Lee, *J. Phys. G* **20**, 1531 (1994); C. Lee, S. N. Yang and T.-S.H. Lee, *ibid. G* **17**, L131 (1991).
22. R. A. Arndt, I. I. Strakovsky and R. L. Workman, *Phys. Rev. C* **53**, 430 (1996).
23. W. W. Ash *et al.*, *Phys. Lett.* **24B**, 165 (1967).
24. F. Foster and G. Hughes, *Rep. Prog. Phys.* **46**, 1445 (1983)( $\bullet$ ); S. Stein *et al.*, *Phys. Rev. D* **12**, 1884 (1975)(black triangle); W. Bartel *et al.*, *Phys. Lett.* **28B**, 148 (1968)( $\circ$ ); K. Bätzner *et al.*, *Phys. Lett.* **39B**, 575 (1972)( $\triangle$ ).
25. <http://www.kph.uni-mainz.de/MAID>.
26. H. F. Jones and M. D. Scadron, *Ann. of Phys.* **81**, 1 (1973).
27. S. Capstick and B. D. Keister, *Phys. Rev. D* **51**, 3598 (1995); R. Bijker, F. Iachello, and A. Levitan, *Ann. Phys.* **236**, 69 (1994); M. Warns, H. Schröder, W. Pfeil and H. Rolnik, *Z. Phys. C* **45**, 627 (1990); V. Keiner, *Z. Phys. A* **359**, 91 (1997).
28. A. J. Buchmann, E. Hernández, and A. Faessler, *Phys. Rev. C* **55** 448 (1997).
29. G. Dillon and G. Morpurgo, *Phys. Lett. B* **448**, 107 (1999).
30. G. Blanpied *et al.*, *Phys. Rev. C* **64** 025203 (2001).
31. V. V. Frolov *et al.*, *Phys. Rev. Lett.* **82**, 45 (1999).
32. K. Joo *et al.*, *Phys. Rev. Lett.* **88**, 122001 (2002).
33. R. A. Arndt, I. I. Strakovsky, and R. L. Workman,  *$\pi N$  Newsletter* **16**, 150 (2002).
34. G. G. Gellas, T. R. Hemmert, C. N. Ktorides, and G. I. Poulis, *Phys. Rev. D* **60**, 054022, (1999).
35. T. Sato and T.-S. H. Lee, *Phys. Rev. C* **63**, 055201 (2001)